General Formulation of the Electromagnetic Field Distribution in Machines and Devices Using Fourier Analysis

B. L. J. Gysen, K. J. Meessen, J. J. H. Paulides, and E. A. Lomonova

Electromechanics and Power Electronics Group, Department of Electrical Engineering, Eindhoven University of Technology, 5600 MB, Eindhoven, The Netherlands

We present a general mesh-free description of the magnetic field distribution in various electromagnetic machines, actuators, and devices. Our method is based on transfer relations and Fourier theory, which gives the magnetic field solution for a wide class of two-dimensional (2-D) boundary value problems. This technique can be applied to rotary, linear, and tubular permanent-magnet actuators, either with a slotless or slotted armature. In addition to permanent-magnet machines, this technique can be applied to any 2-D geometry with the restriction that the geometry should consist of rectangular regions. The method obtains the electromagnetic field distribution by solving the Laplace and Poisson equations for every region, together with a set of boundary conditions. Here, we compare the method with finite-element analyses for various examples and show its applicability to a wide class of geometries.

Index Terms—**Boundary value problem, Fourier analysis, permanent magnet.**

LIST OF SYMBOLS

$\vec{A}$	Magnetic vector potential	$\mathrm{Wb\,m^{-1}}$
$\vec{B}$	Magnetic flux density vector	T
B_{rem}	Remanent flux density	T
$\vec{e}$	Unit vector	-
$\vec{H}$	Magnetic field strength vector	$\mathrm{A\,m^{-1}}$
h	Height	m
$\vec{J}$	Current density vector	$\mathrm{A/m^2}$
k	Region number	-
l	Longitudinal direction	m
$\vec{M}$	Magnetization vector	$\mathrm{A\,m^{-1}}$
m	Harmonic number	—
n	Harmonic number	—
p	Normal direction	m
q	Tangential direction	m
w	Spatial frequency	$\mathrm{m^{-1}\ or\ rad^{-1}}$
χ	Magnetic susceptibility	—
Δ	Offset in tangential direction	m
μ	Permeability	$\mathrm{H\,m^{-1}}$
μ_0	Permeability of vacuum	$\mathrm{H\,m^{-1}}$
μ_r	Relative permeability	—
θ	Angular direction	rad
τ	Width	m or rad
$\mathcal{I}_0$	Bessel function of first kind of 0th order	—
$\mathcal{I}_1$	Bessel function of first kind of 1th order	—
$\mathcal{K}_0$	Bessel function of second kind of 0th order	—
$\mathcal{K}_1$	Bessel function of second kind of 1th order	—

I. INTRODUCTION

EXTENSIVE modeling of the electromagnetic field distribution has become a crucial step in the design process for developing electromagnetic devices, machines, and actuators which have improved position accuracy, acceleration, and force density. During recent years, a lot of research and development has been conducted to be able to model or predict the magnetic field distribution in electromagnetic structures. Several analytical, semianalytical, and numerical techniques exist in the literature:

- the magnetic equivalent circuit (MEC) [1], [2];
- the charge model (CM) [3], [4];
- transfer relations—Fourier analysis (TR-FA) [5]–[8];
- Schwarz-Christoffel conformal mapping (SC) [9]–[12];
- finite-element method (FEM) [13];
- boundary-element method (BEM) [14].

In general, each type of problem will have its own optimal modeling technique, since high accuracy is not always preferred and a low computational time could be more important. For almost every technique, these requirements are a tradeoff, although the increased computational capability of microprocessors enhanced the use of numerical methods. A large class of the mentioned methods (MEC, SC, FEM, FEM, amd BEM) require geometry discretization, mesh, prior to the calculation of the electromagnetic field distribution; hence, only solutions at the predefined points are obtained. An increased mesh density improves the accuracy, but also increases the computational time. Additionally, correct geometry discretization requires prior knowledge to get a reliable solution. In ironless structures, without concentrated magnetic fields, or machines with a small air gap and a large outer size, these methods become even more problematic due to the necessity of a high mesh density and/or size.

For analytical or numerical calculation of secondary parameters, like force, electromotive force, or inductance, only the field solution at a predetermined point or "line" is necessary. Numerical methods require the solution for the total meshed geometry in order to obtain these secondary parameters [15]–[17].

Therefore, a mesh-free solution is preferred since the computational time reduces and, in certain problems, it even allows for analytical expressions which provide for direct means to illustrate the dependencies of the geometric parameters and material properties.

This paper will discuss the analytical calculation of the electromagnetic fields using transfer relations and Fourier analysis. The direct solution of the magnetostatic Maxwell equations is considered, which reduces to the Laplace equation in the air region and the Poisson equation in a magnet or current carrying region. This method originates from the book of Hague [5], which only considers the field solution for arbitrary positioned current carrying wires between two parallel or concentric iron surfaces. Boules [7] applied this work for permanent magnets by replacing them by an equivalent distribution of ampere-conductors and using Hague's field solution. The disadvantage is that no irregular iron shapes can be considered and that the magnet should have a simple geometric shape and magnetization direction. The solutions of the Maxwell equations including permanent magnets described by harmonic series were published by Zhu *et al.* [8]. Recently, several publications extended this method considering specific problems in different coordinate systems [18]–[24].

In this paper, the method is extensively described in a generalized manner, focusing on:

- model formulation;
- methodology;
- general field solutions in two-dimensional (2-D) coordinate systems;
- examples in 2-D coordinate systems (FEM comparison);
- numerical limitations.

The model formulation can be applied for general 2-D problems in the Cartesian, polar, and cylindrical coordinate system. The distinction between regions with periodical boundary conditions and Neumann boundary conditions in the tangential direction is made. Therefore, irregular rectangular iron shapes can be considered; hence, a wide range of devices can be modeled using this technique. Examples of the analytical solution for the three coordinate systems are compared with 2-D finite-element analysis (Cedrat FLUX2D [25]). Furthermore, numerical problems and drawbacks for certain conditions will be addressed.

II. MODEL FORMULATION

A. Model Assumptions

To obtain a semianalytical field solution, the following assumptions have to be made:

1) the problem can be described by a 2-D model;
2) the materials are linear;
3) the materials are homogeneous;
4) the soft-magnetic material (iron) is infinite permeable;
5) source terms are invariant in the normal direction within one region.

General electromagnetic devices have a 3-D geometry. Since only 2-D problems can be considered, the geometry should be invariant with one of the three dimensions, or its dependency should be negligible. In general, this is a valid assumption since

TABLE I
COORDINATE SYSTEMS

	Normal	Tangential	Longitudinal
General	p	q	l
Cartesian	y	x	z
Polar	r	θ	z
Cylindrical	r	z	θ

for example, in rotary actuators the 3-D effects due to the finite axial length are often negligible, and in tubular actuators, the axisymmetry results inherently in a 2-D problem description. A large class of long-stroke actuators and machines exhibit a certain symmetry or periodicity. The use of Fourier theory allows one to use that periodicity to describe the magnetic field distribution. If the 2-D problem has no periodicity, it can be obtained by repeating the problem in the direction where the periodicity should be obtained with the assumption that the electromagnetic influence of the repetition on the 2-D problem is negligible. Three different 2-D coordinate systems will be considered: Cartesian (x, y), polar (r, θ), and cylindrical (r, z). The direction of periodicity is arbitrary for the Cartesian coordinate system; either the x- or the y-direction can be used, however, the x-direction is chosen in this paper. For the polar and cylindrical coordinate system, the direction of periodicity is the θ- and z-direction, respectively, since physically no electromagnetic periodicity can be obtained in the r-direction. For generality the normal direction is referred as the p-direction, the direction of periodicity or the tangential direction is referred as the q-direction, and the longitudinal (invariant) direction is referred as the l-direction. A summary of the considered coordinate systems is given in Table I.

The analytical solution only applies to linear problems; hence, the permeability of all materials is assumed to be isotropic and homogenous. The permanent magnets are modeled with a linear B-H magnetization curve in the second quadrant with remanence B_{rem} and relative recoil permeability μ_r.

The relative permeability of the soft-magnetic material is assumed to be infinite; hence, the magnetic field distribution is not calculated inside the soft-magnetic material but the magnetic field strength normal to the boundary of the soft-magnetic material is set to zero (Neumann boundary condition).

The source regions, magnets or current carrying coils, are invariant in the normal direction. This implies that a source that varies in the normal direction should be described by multiple regions [23].

B. Examples

For every coordinate system, an example will be given which indicates the applicability of the proposed method. For the Cartesian coordinate system a structure enclosed with soft-magnetic material is considered which has an irregular rectangular shape, Fig. 1. This indicates that the model is even applicable to structures enclosed by soft-magnetic material without periodicity. The example in the polar coordinate system is a three-phase rotary brushless permanent-magnet actuator with slotted stator, Fig. 2, indicating the ability of
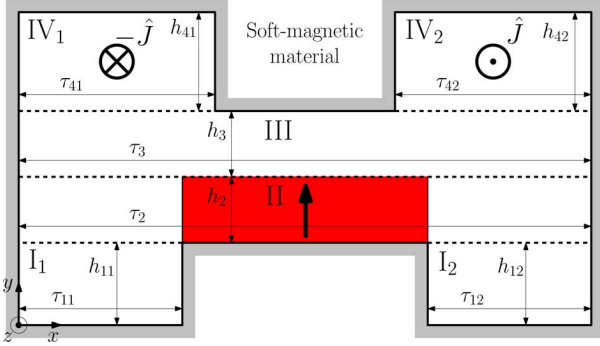
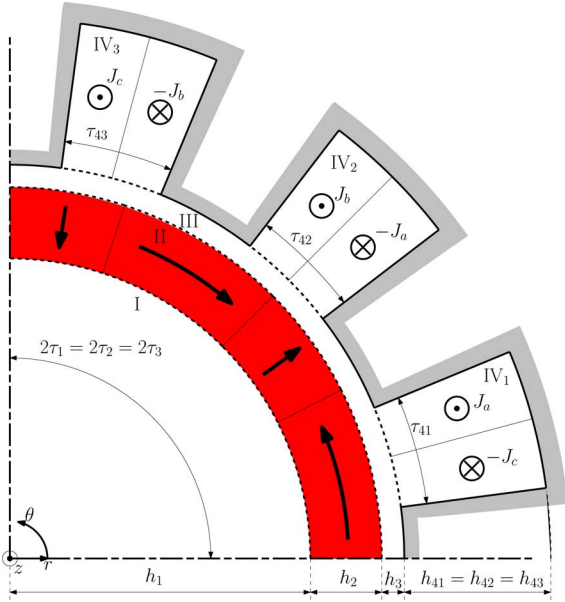Fig. 1. Boundary value problem in the Cartesian coordinate system.

Fig. 2. Boundary value problem in the polar coordinate system, a three-phase slotted brushless PM actuator.
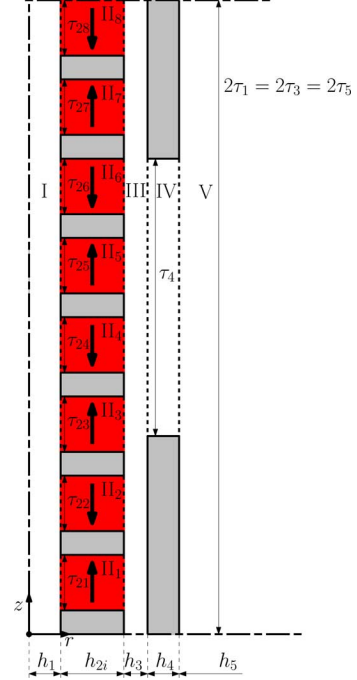
modeling slotted permanent-magnet actuators in a semianalytical manner. For the cylindrical coordinate system, a slotless tubular permanent-magnet actuator with axial magnetization is modeled, Fig. 3. In that particular example, the field distribution due to a finite stator length will be calculated which allows for cogging force calculation, as discussed in [21] for radial and Halbach magnetization.

C. Division in Regions

In order to solve the total field distribution in the electromagnetic actuator or device, the 2-D geometry will be divided into several regions. Since the soft-magnetic materials are assumed to have infinite permeability, three different regions are considered:

- source-free regions (air, vacuum);
- magnetized regions (permanent magnets);
- current carrying regions (coils, wires).

Every region should be enclosed by four boundaries where each boundary is in parallel with one of the two variant dimensions under consideration (normal or tangential). When a boundary is

Fig. 3. Boundary value problem in the cylindrical coordinate system, a slotless tubular PM actuator.

not in parallel with one of the two dimensions, it can be approximated by a finite number of rectangles with varying length [23]. The division in and number of regions defines the form of the solution and the complexity of the problem. For the examples considered, a number of 6, 7, and 12 regions is necessary to model the boundary value problem for the Cartesian (Fig. 1), polar (Fig. 2), and cylindrical (Fig. 3) coordinate system, respectively.

To simplify the magnetic field formulation, each region has a local coordinate system. The main coordinate system is (p,q), where the local coordinate system (p,q_k) for every region is defined as

$$q_k = q - \Delta_k \tag{1}$$

where the offset Δ_k is indicated in Figs. 4 and 5.

D. Motion

Since all regions have a parameter Δ_k defining the offset in the tangential direction, motion in this direction can easily be implemented. Defining a set of fixed regions and a set of moving regions, an increment of the parameter Δ_k for all regions within the moving set results in a positive displacement. Now it is possible to calculate the field distribution for all positions of the moving part.

E. Boundary Value Problem

Dividing the geometry in regions results in a boundary value problem. This type of problem has three types of boundary conditions: periodic, Neumann, and continuous. The boundaries of a region parallel to the p-direction should both be periodic (Fig. 4) or Neumann (Fig. 5). The boundaries parallel to the
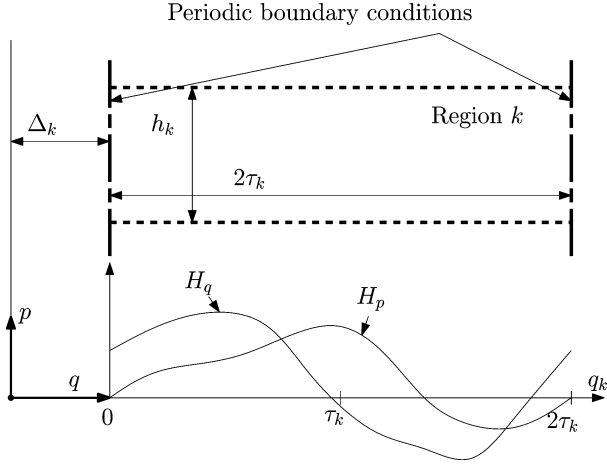
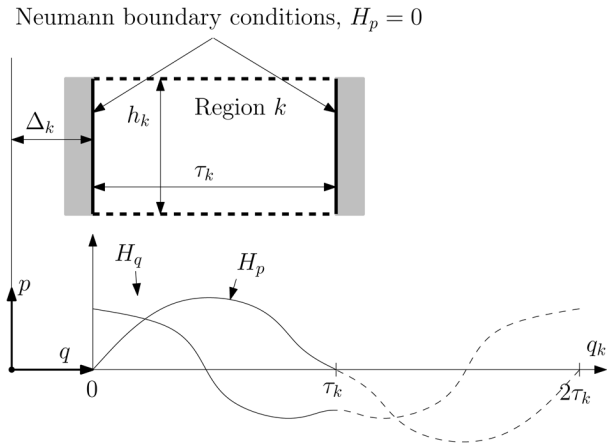Fig. 4. Definition of a region with periodic boundaries.

Fig. 5. Definition of a region with Neumann boundaries.

q-direction can either be Neumann or continuous or a combination of both. The division in regions is such that each region has constant permeability and the source term does not vary in the normal direction.

The reason for applying Fourier theory to the solution of the magnetic field distribution is to satisfy the boundary conditions in the tangential direction (constant p).

For a region with periodic boundary conditions, Fig. 4, and width $2\tau_k$, choosing the mean period of $2\tau_k$ for the Fourier series of the magnetic field inherently satisfies the periodic boundary conditions.

For a region with soft-magnetic boundaries, Fig. 5, the tangential magnetic field component at the boundary has to be zero. As a sine function has two zero crossings (at 0 and π), describing the component of the magnetic field tangential to the boundary by means of a Fourier series with mean period $2\tau_k$, where τ_k is the width of the region, inherently satisfies the Neumann boundary condition ($H_p = 0$).

The boundary conditions in the normal direction (constant q) will result in a set of equations which are used to solve the unknown coefficients of the magnetic field description which will be discussed in Section IV.

III. SEMIANALYTICAL SOLUTION

A. Magnetostatic Maxwell Equations

In order to solve the magnetostatic field distribution, the magnetic flux density can be written in terms of the magnetic vector potential $\vec{A}$ as

$$\vec{B} = \nabla \times \vec{A} \tag{2}$$

since $\nabla \cdot \vec{B} = 0$. For the remainder of this paper, the definition of the magnetization vector $\vec{M}$ as employed by Zhu [8] will be used wherein

$$\vec{M} = \chi \vec{H} + \vec{M}_0 \tag{3}$$

$$\vec{M}_0 = \frac{\vec{B}_{\text{rem}}}{\mu_0} \tag{4}$$

with χ the magnetic susceptibility and $\vec{M}_0$ the residual magnetization. This definition of the magnetization vector gives the constitutive relation in the form of

$$\vec{B} = \mu_0(\vec{H} + \vec{M}) \tag{5}$$

$$= \mu_0 \mu_r \vec{H} + \mu_0 \vec{M}_0 \tag{6}$$

where $\mu_r = (1+\chi)$ is the relative permeability of the considered region k. This reduces the magnetostatic Maxwell equations to a Poisson equation for every region k, given by

$$\nabla^2 \vec{A} = -\mu_0(\nabla \times \vec{M}_0) - \mu \vec{J} \tag{7}$$

with $\mu = \mu_0 \mu_r$. Since only 2-D boundary value problems are considered, the magnetization vector $\vec{M}_0$ only has components in the normal (M_p) and tangential direction (M_q) and the current density vector $\vec{J}$ has only a component in the longitudinal direction (J_l). Therefore, the magnetic vector potential has only a component in the longitudinal direction (A_l) which is only dependent on the normal (p) and tangential direction (q). The Poisson equations in the different coordinate systems are therefore given by

Cartesian :

$$\frac{\partial^2 A_l}{\partial p^2} + \frac{\partial^2 A_l}{\partial q^2} = -\mu_0 \left(\frac{\partial M_p}{\partial q} - \frac{\partial M_q}{\partial p} \right) - \mu J_l \tag{8}$$

Polar:

$$\frac{1}{p} \frac{\partial}{\partial p} p \frac{\partial A_l}{\partial p} + \frac{1}{p^2} \frac{\partial^2 A_l}{\partial q^2} = -\mu_0 \left(\frac{1}{p} \frac{\partial(p M_q)}{\partial p} - \frac{1}{p} \frac{\partial M_p}{\partial q} \right) - \mu J_l \tag{9}$$

Cylindrical:

$$\frac{1}{p} \frac{\partial}{\partial p} p \frac{\partial A_l}{\partial p} + \frac{\partial^2 A_l}{\partial q^2} - \frac{1}{p^2} A_l = -\mu_0 \left(\frac{\partial M_p}{\partial q} - \frac{\partial M_q}{\partial p} \right) - \mu J_l. \tag{10}$$

Note that when a particular region k is considered, the local coordinate systems need to be considered by replacing q by q_k. The magnetic flux density distribution can be obtained from the solution of the magnetic vector potential by means of (2) and

the magnetic field strength $\left(\vec{H}\right)$ is obtained from the flux density distribution by means of the constitutive relation (6).

B. Source Term Description

The description of the Fourier series for the source terms is different for regions with periodical boundary conditions in the tangential direction than for region with Neumann boundary conditions in the tangential direction, see Figs. 4 and 5. The function which describes the source term, magnet or coil region, will be assigned as f, which can be the normal (M_p) or tangential magnetization component (M_q), or the longitudinal current density component (J_l)

$$\vec{M}_0 = M_p \vec{e}_p + M_q \vec{e}_q \tag{11}$$

$$M_p = M_{p_0} + \sum_{n=1}^{\infty} (M_{ps} \sin(w_k q_k) + M_{pc} \cos(w_k q_k)) \tag{12}$$

$$M_q = M_{q_0} + \sum_{n=1}^{\infty} (M_{qs} \sin(w_k q_k) + M_{qc} \cos(w_k q_k)) \tag{13}$$

$$\vec{J} = J_l \vec{e}_l \tag{14}$$

$$J_l = J_{l_0} + \sum_{n=1}^{\infty} (J_{ls} \sin(w_k q_k) + J_{lc} \cos(w_k q_k)) \tag{15}$$

where the spatial frequencies w_k for every region k are defined as

$$w_k(n) = \frac{n\pi}{\tau_k}. \tag{16}$$

For regions k with periodical boundary conditions, the width of the region is defined as $2\tau_k$. Hence, using general Fourier theory, the source function f as function of the tangential direction q_k for region k can be written in terms of Fourier series as

$$f = f_0 + \sum_{n=1}^{\infty} (f_s \sin(w_k q_k) + f_c \cos(w_k q_k)) \tag{17}$$

$$f_0 = \frac{1}{2\tau_k} \int_0^{2\tau_k} f \, dq_k \tag{18}$$

$$f_s(n) = \frac{1}{\tau_k} \int_0^{2\tau_k} f \sin(w_k q_k) dq_k \tag{19}$$

$$f_c(n) = \frac{1}{\tau_k} \int_0^{2\tau_k} f \cos(w_k q_k) dq_k. \tag{20}$$

For regions with Neumann boundary conditions, the width of the region is defined as τ_k, but the main period of the Fourier series for the source term is still $2\tau_k$. The total source description is therefore obtained by applying the imaging method [5], where the source is mirrored around its tangential boundaries as indicated in Fig. 6. A consequence of this imaging method is that, for normal magnetized regions, the cosine terms will be zero $(M_{pc} = 0)$ and, for the tangential magnetized regions and longitudinal current density regions, the sine terms will be zero $(M_{qs} = 0, J_{ls} = 0)$. After applying the imaging method, (17) to (20) can still be applied.
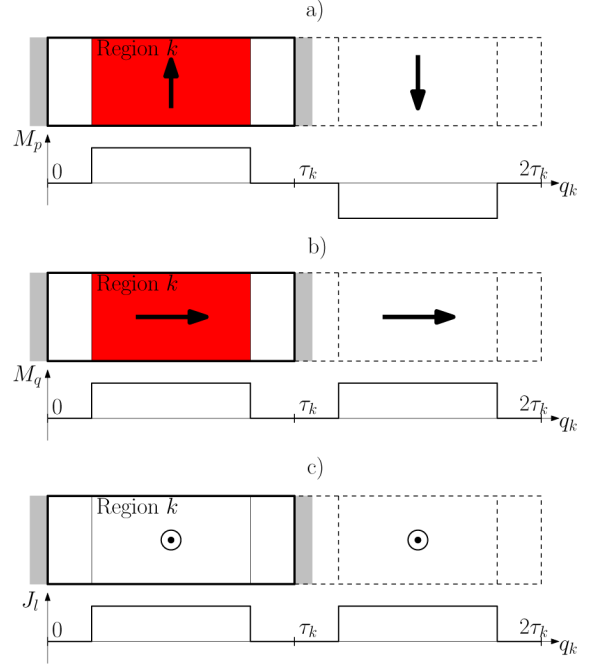

Fig. 6. Source description for regions with Neumann boundary conditions in tangential direction. (a) Normal magnetized region. (b) Tangential magnetized region. (c) Longitudinal current source region.

C. Semianalytical Solution

Since the source terms are expressed by means of Fourier analysis, the resulting solution for the magnetic vector potential is also written in terms of Fourier components. The Poisson equation is solved with the use of separation of variables, hence the solution for the vector magnetic potential is given by a product of two functions, one dependent on the normal direction (p) and one on the tangential direction (q). As mentioned before, the functions for the tangential direction are sine and cosine functions since a Fourier description is used. The function for the normal direction is such that the Poisson equation is satisfied

$$\vec{A} = A_l(p, q_k)\vec{e}_l \tag{21}$$

$$A_l = \sum_{n=1}^{\infty} (A_{ps}(p) \sin(w_k q_k) + A_{pc}(p) \cos(w_k q_k)) + A_{l_0}(p). \tag{22}$$

Hence, the expressions for the magnetic flux density distribution can generally be written as

$$\vec{B} = B_p(p, q_k)\vec{e}_p + B_q(p, q_k)\vec{e}_q \tag{23}$$

$$B_p = \sum_{n=1}^{\infty} (B_{ps}(p) \sin(w_k q_k) + B_{pc}(p) \cos(w_k q_k)) \tag{24}$$

$$B_q = \sum_{n=1}^{\infty} (B_{qs}(p) \sin(w_k q_k) + B_{qc}(p) \cos(w_k q_k)) + B_{q_0}(p) \tag{25}$$

where the functions B_{ps}, B_{pc}, B_{qs}, B_{qc}, and B_{q_0} can be obtained by considering the transfer relations for every coordinate system [6], and are given by

1) Cartesian Coordinate System:

$$B_{ps} = a_n e^{w_k\,p} + b_n e^{-w_k\,p} + G_{ps} \tag{26}$$

$$B_{pc} = -c_n e^{w_k\,p} - d_n e^{-w_k\,p} + G_{pc} \tag{27}$$

$$B_{qs} = c_n e^{w_k\,p} - d_n e^{-w_k\,p} \tag{28}$$

$$B_{qc} = a_n e^{w_k\,p} - b_n e^{-w_k\,p} \tag{29}$$

$$B_{q_0} = -\mu J_{l_0} p + B_0 \tag{30}$$

where G_{ps} and G_{pc} are defined as

$$G_{ps} = \mu_0 M_{ps} + \frac{\mu J_{lc}}{w_k} \tag{31}$$

$$G_{pc} = \mu_0 M_{pc} - \frac{\mu J_{ls}}{w_k}. \tag{32}$$

2) Polar Coordinate System:

$$B_{ps} = a_n p^{w_k-1} + b_n p^{-w_k-1} + G_{ps} \tag{33}$$

$$B_{pc} = -c_n p^{w_k-1} - d_n p^{-w_k-1} + G_{pc} \tag{34}$$

$$B_{qs} = c_n p^{w_k-1} - d_n p^{-w_k-1} + G_{qs} \tag{35}$$

$$B_{qc} = a_n p^{w_k-1} - b_n p^{-w_k-1} + G_{qc} \tag{36}$$

$$B_{q_0} = \frac{1}{2}\mu J_{l_0} p + \mu_0 M_{q_0} - \frac{A_0}{p} \tag{37}$$

where G_{ps}, G_{pc}, G_{qc}, and G_{qs} are defined as

$$G_{ps} = \begin{cases} -\mu_0 \frac{M_{ps}-M_{qc}}{2}\ln(p) + \mu\frac{J_{lc}}{3}p, & w_k = 1, \\ \mu_0 \frac{4M_{ps}-2M_{qc}}{3} + \mu\frac{J_{lc}}{2}p\ln(p), & w_k = 2, \\ \mu_0 w_k \frac{w_k M_{ps}-M_{qc}}{w_k^2-1} + \mu w_k \frac{J_{lc}}{w_k^2-4}p, & \text{else} \end{cases} \tag{38}$$

$$G_{pc} = \begin{cases} -\mu_0 \frac{M_{pc}+M_{qs}}{2}\ln(p) - \mu\frac{J_{ls}}{3}p, & w_k = 1, \\ \mu_0 \frac{4M_{pc}+2M_{qs}}{3} - \mu\frac{J_{ls}}{2}p\ln(p), & w_k = 2, \\ \mu_0 w_k \frac{w_k M_{pc}+M_{qs}}{w_k^2-1} - \mu w_k \frac{J_{ls}}{w_k^2-4}p, & \text{else} \end{cases} \tag{39}$$

$$G_{qs} = \begin{cases} \mu_0 \frac{M_{pc}+M_{qs}}{2}(1+\ln(p)) + \mu\frac{2J_{ls}}{3}p, & w_k = 1, \\ -\mu_0 \frac{2M_{pc}+M_{qs}}{3} + \mu\frac{J_{ls}}{4}p(1+2\ln(p)), & w_k = 2, \\ -\mu_0 \frac{w_k M_{pc}+M_{qs}}{w_k^2-1} + \mu\frac{2J_{ls}}{w_k^2-4}p, & \text{else} \end{cases} \tag{40}$$

$$G_{qc} = \begin{cases} -\mu_0 \frac{M_{ps}-M_{qc}}{2}(1+\ln(p)) + \mu\frac{2J_{lc}}{3}p, & w_k = 1, \\ \mu_0 \frac{2M_{ps}-M_{qc}}{3} + \mu\frac{J_{lc}}{4}p(1+2\ln(p)), & w_k = 2, \\ \mu_0 \frac{w_k M_{ps}-M_{qc}}{w_k^2-1} + \mu\frac{2J_{lc}}{w_k^2-4}p, & \text{else}. \end{cases} \tag{41}$$

Cylindrical Coordinate System:

$$B_{ps} = a_n \mathcal{I}_1(w_k\,p) + b_n \mathcal{K}_1(w_k\,p) + G_{ps} \tag{42}$$

$$B_{pc} = -c_n \mathcal{I}_1(w_k\,p) - d_n \mathcal{K}_1(w_k\,p) + G_{pc} \tag{43}$$

$$B_{qc} = a_n \mathcal{I}_0(w_k\,p) - b_n \mathcal{K}_0(w_k\,p) + G_{qc} \tag{44}$$

$$B_{qs} = c_n \mathcal{I}_0(w_k\,p) - d_n \mathcal{K}_0(w_k\,p) + G_{qs} \tag{45}$$

$$B_{q_0} = -\mu J_{l_0} p + B_0 \tag{46}$$

where G_{ps}, G_{pc}, G_{qs}, and G_{qc} are defined as

$$G_{ps} = \left(\mu_0 M_{ps} + \mu\frac{J_{lc}}{w_k}\right) F_p \tag{47}$$

$$G_{pc} = \left(\mu_0 M_{pc} - \mu\frac{J_{ls}}{w_k}\right) F_p \tag{48}$$

$$G_{qs} = \left(\mu_0 M_{pc} - \mu\frac{J_{ls}}{w_k}\right) F_q \tag{49}$$

$$G_{qc} = -\left(\mu_0 M_{ps} + \mu\frac{J_{lc}}{w_k}\right) F_q \tag{50}$$

and F_p and F_q are defined as

$$F_p = \mathcal{K}_1(w_k\,p)\int_0^{w_k\,p}\mathcal{I}_1(\nu)\nu d\nu - \mathcal{I}_1(w_k\,p)\int_0^{w_k\,p}\mathcal{K}_1(\nu)\nu d\nu \tag{51}$$

$$F_q = \mathcal{K}_0(w_k\,p)\int_0^{w_k\,p}\mathcal{I}_1(\nu)\nu d\nu + \mathcal{I}_0(w_k\,p)\int_0^{w_k\,p}\mathcal{K}_1(\nu)\nu d\nu. \tag{52}$$

For regions with Neumann boundary conditions in the tangential direction, Fig. 5, H_p should be zero at the tangential boundaries of the region; consequently, B_p only contains sine terms ($B_{pc} = 0$). Since the normal and tangential component of the magnetic flux density are linked via the magnetic vector potential, the sine terms of the tangential component will also be zero in that case ($B_{qs} = 0$).

The set of unknowns a_n, b_n, c_n, d_n, and B_0 or A_0 for every region are solved considering the boundary conditions in the normal direction which will be discussed in the following section.

IV. BOUNDARY CONDITIONS

Due to the proper choice of the solution form for the magnetic flux density distribution, the boundary conditions in the tangential direction are inherently satisfied as discussed in Section II. To solve the unknown coefficients in the set of solutions for the magnetic flux density distribution, the boundary conditions in the normal direction have to be considered. Five types of boundary conditions can be distinguished:

- Neumann boundary conditions;
- continuous boundary conditions;
- combination of Neumann and continuous boundary conditions;
- conservation of magnetic flux;
- Ampère's law.

Each of them will be considered in the following subsections.

A. Neumann Boundary Condition

A Neumann boundary condition (tangential magnetic field strength must be zero) appears at the normal interface between a region k and a soft-magnetic material at a certain height $p = h_b$, as shown in Fig. 7

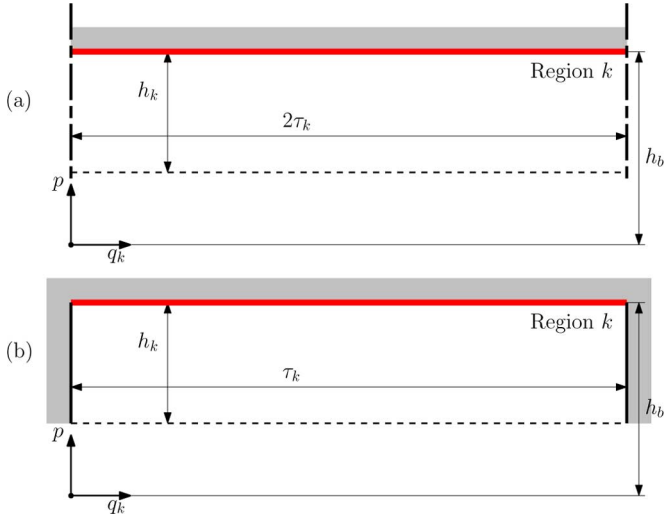$$H_{q_k} = 0|_{p=h_b}. \tag{53}$$

Fig. 7. Neumann boundary condition for a region k with (a) periodic boundary conditions and (b) Neumann boundary conditions in the tangential direction.

Using the constitutive relation (6), (53) can be written in terms of the magnetic flux density and magnetization as

$$B_{q_k} - \mu_0 M_{q_k} = 0|_{p=h_b}. \tag{54}$$

Equation (54) implies that the sum of a Fourier series needs to be zero at height $p = h_b$ for all q_k. This can be obtained if every harmonic term of the Fourier series is zero including the dc term; hence, both the coefficients for the sine and cosine terms need to be zero as well as the dc term. Equation (54) can therefore be rewritten in the following set of equations for every harmonic n:

$$B_{qs_k} - \mu_0 M_{qs_k} = 0|_{p=h_b} \tag{55}$$
$$B_{qc_k} - \mu_0 M_{qc_k} = 0|_{p=h_b} \tag{56}$$
$$B_{q0_k} - \mu_0 M_{q0_k} = 0|_{p=h_b}. \tag{57}$$

B. Continuous Boundary Condition

For the continuous boundary condition, the normal component of the magnetic flux density $(\vec{B})$ needs to be continuous as well as the tangential component of the magnetic field strength $(\vec{H})$ at the boundary between region k and j giving

$$B_{p_k} = B_{p_j}|_{p=h_b} \tag{58}$$
$$H_{q_k} = H_{q_j}|_{p=h_b}. \tag{59}$$

Using the constitutive relation (5), (59) can be written in terms of the magnetic flux density as

$$\mu_j(B_{q_k} - \mu_0 M_{q_k}) = \mu_k(B_{q_j} - \mu_0 M_{q_j})|_{p=h_b}. \tag{60}$$

The two regions (k and j) have the same width and equal offsets $(\Delta_k = \Delta_j)$, as shown in Fig. 8. This implies that both regions have the same spatial frequencies $(w_k(n) = w_j(n))$ and the same coordinate systems $(q_k = q_j)$. Applying (58) and (60) to the flux density distributions at the boundary height $(p = h_b)$ will result in equating two Fourier series with equal fundamental frequency. Consequently (58) and (60) should hold for every
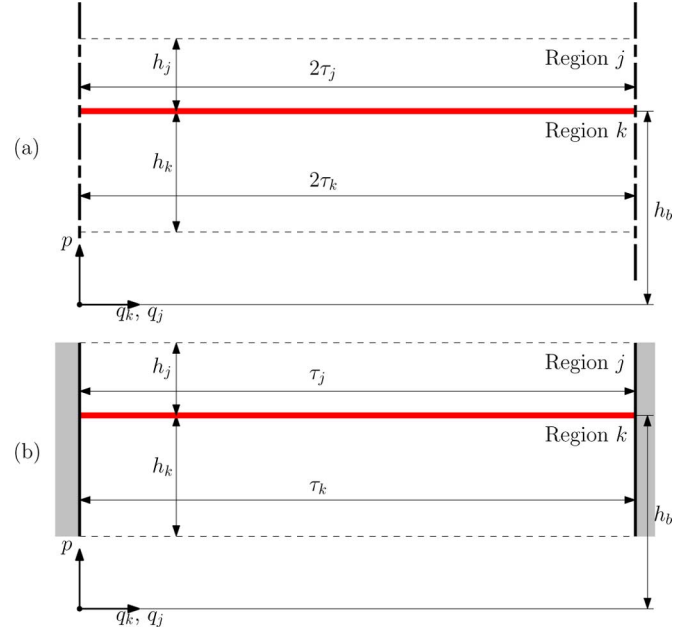

Fig. 8. Continuous boundary condition between a region k and j with (a) periodic boundary conditions and (b) Neumann boundary conditions in the tangential direction.

harmonic; hence, the coefficients for both the sine and the cosine function should be equal as well as the dc terms.

Equation (58) will give the following set of equations for every harmonic n:

$$B_{ps_k} = B_{ps_j}|_{p=h_b} \tag{61}$$
$$B_{pc_k} = B_{pc_j}|_{p=h_b}. \tag{62}$$

The boundary condition for the continuous tangential magnetic field strength (60) will result in the following set of equations for every harmonic n:

$$\frac{\mu_j}{\mu_k}(B_{qs_k} - \mu_0 M_{qs_k}) = B_{qs_j} - \mu_0 M_{qs_j}|_{p=h_b} \tag{63}$$
$$\frac{\mu_j}{\mu_k}(B_{qc_k} - \mu_0 M_{qc_k}) = B_{qc_j} - \mu_0 M_{qc_j}|_{p=h_b} \tag{64}$$
$$\frac{\mu_j}{\mu_k}(B_{q0_k} - \mu_0 M_{q0_k}) = B_{q0_j} - \mu_0 M_{q0_j}|_{p=h_b}. \tag{65}$$

C. Combination of a Neumann and Continuous Boundary Condition

A combination of Neumann and continuous boundary conditions occurs at an interface between regions which have unequal width and/or unequal offsets. In general, it concerns the boundary condition at height $p = h_b$, between a region k on one side, and one or more regions $j_1, j_2, \ldots, j_V$, on the other side. A general example for $V = 2$ is shown in Fig. 9(a) where region k has periodic boundary conditions in tangential direction and Fig. 9(b) where region k has Neumann boundary conditions in tangential direction. The region j_v will always have Neumann boundary conditions in the tangential direction. The technique for solving this type of boundary conditions is for example discussed in [18], [22]. The normal magnetic flux density component B_p of every region j_v should equal the normal magnetic field component of region k on the boundary at $p = h_b$.
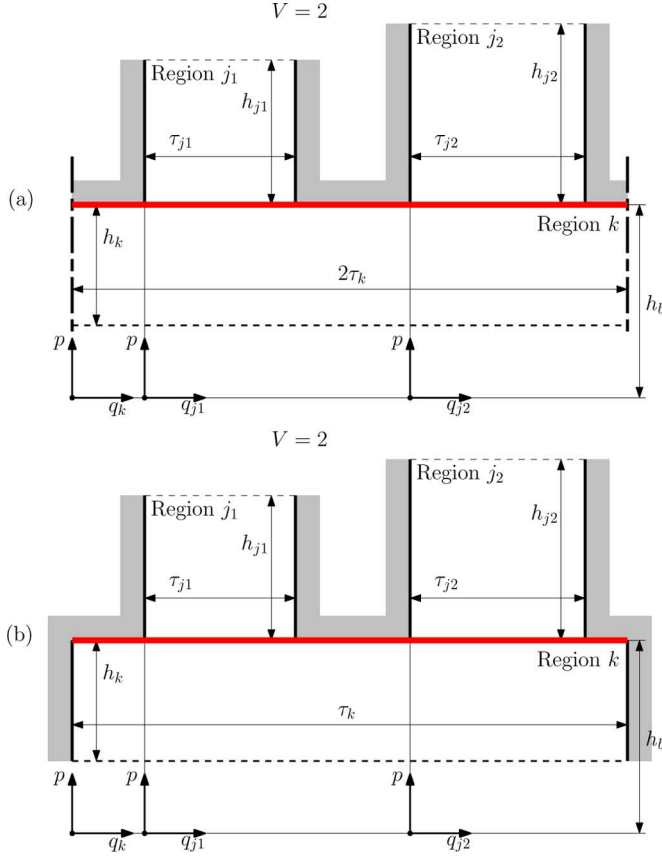
Fig. 9. Boundary condition between regions j_1, j_2, and k with (a) periodic boundary conditions and (b) Neumann boundary conditions in the tangential direction.

Furthermore, the tangential magnetic field strength component H_q of region k must equal the tangential magnetic field strength component of every region j_v on the respective boundary, and equal zero elsewhere. Therefore, the boundary conditions are rewritten in the form

$$B_{p_{j_v}} = B_{p_k}|_{p=h_b}, \quad 0 \le q_{j_v} \le \tau_{j_v}, \quad \text{for } v = 1, \dots, V \quad (66)$$

$$H_{q_k} = \begin{cases} \sum_{v=1}^{V} H_{q_{j_v}}|_{p=h_b}, & 0 \le q_{j_v} \le \tau_{j_v}, \\ 0, & \text{else.} \end{cases} \quad (67)$$

Applying the constitutive relation (5) to (67) gives

$$\left(B_{q_k} - \mu_0 M_{q_k} \right) = \begin{cases} \sum_{v=1}^{V} \frac{\mu_k}{\mu_{j_v}} (B_{q_{j_v}} - \mu_0 M_{q_{j_v}})|_{p=h_b}, & 0 \le q_{j_v} \le \tau_{j_v}, \\ 0, & \text{else.} \end{cases} \quad (68)$$

Boundary condition (66) implies that two waveforms which have a different fundamental frequency should be equal for a certain interval. Boundary condition (68) implies that a waveform should be equal to another waveform with different fundamental frequency and zero elsewhere. Both boundary conditions are solved using the correlation technique which will be described in the following subsections.

1) Normal Magnetic Flux Density: Substituting the general functions for the magnetic flux density distribution in (66) gives the following V equations:

$$\sum_{m=1}^{\infty} \left(B_{ps_{j_v}} \sin \left(w_{j_v} q_{j_v} \right) + B_{pc_{j_v}} \cos(w_{j_v} q_{j_v}) \right)$$
$$= \sum_{n=1}^{\infty} \left(B_{ps_k} \sin(w_k q_k) + B_{pc_k} \cos(w_k q_k) \right)|_{p=h_b}, \quad 0 \le q_{j_v} \le \tau_{j_v}$$
$$\text{for } v = 1, \dots, V. \quad (69)$$

However, this equation has to be rewritten into an infinite number of equations in order to solve the infinite number of unknowns. Therefore, the coefficients of region j_v are written as a function of the coefficients of region k. This can be obtained by correlating (69) with $\sin(w_{j_v} q_{j_v})$ and $\cos(w_{j_v} q_{j_v})$, respectively, over the interval where the boundary condition holds. Since the correlation on the left-hand side is only nonzero for the harmonic m that is considered for the sine or cosine term, respectively, the summation over m disappears giving

$$B_{ps_{j_v}} = \sum_{n=1}^{\infty} \left(B_{ps_k} \varepsilon_s(m,n) + B_{pc_k} \varepsilon_c(m,n) \right),$$
$$\text{for } p = h_b \text{ and } v = 1, \dots, V \quad (70)$$

$$B_{pc_{j_v}} = \sum_{n=1}^{\infty} \left(B_{ps_k} \eta_s(m,n) + B_{pc_k} \eta_c(m,n) \right),$$
$$\text{for } p = h_b \text{ and } v = 1, \dots, V \quad (71)$$

which is a set of equations for every m and region v where the correlation functions ε_s, ε_c, η_s, and η_c are given by

$$\varepsilon_s(m,n) = \frac{2}{\tau_{j_v}} \int_0^{\tau_{j_v}} \sin(w_k q_k) \sin(w_{j_v} q_{j_v}) dq_{j_v} \quad (72)$$

$$\varepsilon_c(m,n) = \frac{2}{\tau_{j_v}} \int_0^{\tau_{j_v}} \cos(w_k q_k) \sin(w_{j_v} q_{j_v}) dq_{j_v} \quad (73)$$

$$\eta_s(m,n) = \frac{2}{\tau_{j_v}} \int_0^{\tau_{j_v}} \sin(w_k q_k) \cos(w_{j_v} q_{j_v}) dq_{j_v} \quad (74)$$

$$\eta_c(m,n) = \frac{2}{\tau_{j_v}} \int_0^{\tau_{j_v}} \cos(w_k q_k) \cos(w_{j_v} q_{j_v}) dq_{j_v}. \quad (75)$$

The solutions of these integrals are given in the Appendix.

2) Tangential Magnetic Field Strength: Substituting the general functions for the magnetic flux density distribution in (68) gives the following single equation:

$$\sum_{n=1}^{\infty} [(B_{qs_k} - \mu_0 M_{qs_k}) \sin(w_k q_k) + (B_{qc_k} - \mu_0 M_{qc_k}) \cos(w_k q_k)] + B_{q_0} - \mu_0 M_{q_{0k}}$$
$$= \begin{cases} \sum_{v=1}^{V} \frac{\mu_k}{\mu_{j_v}} \left[\sum_{m=1}^{\infty} \left[(B_{qs_{j_v}} - \mu_0 M_{qs_{j_v}}) \sin(w_{j_v} q_{j_v}) \right. \right. \\ \left. + \left(B_{qc_{j_v}} - \mu_0 M_{qc_{j_v}} \right) \cos(w_{j_v} q_{j_v}) \right] \\ \left. + B_{q_{0j_v}} - \mu_0 M_{q_{0j_v}} \right]|_{p=h_b}, \quad 0 \le q_{j_v} \le \tau_{j_v}, \\ 0, \quad \text{elsewhere.} \end{cases} \quad (76)$$

However, this equation has to be rewritten into an infinite number of equations in order to solve the infinite number of unknowns. Therefore, the coefficients of region k are written as a function of the coefficients of region j_v. This can be obtained by correlating (76) with $\sin(w_k q_k)$ and $\cos(w_k q_k)$, respectively, over the interval where the boundary condition holds (width of region k). The conditional (76) can be written into an unconditional one by changing the bounds of the right-hand-side correlation integrals into the bounds where the boundary condition holds. Since the correlation on the left-hand side is only nonzero for the harmonic n that is considered for the sine or cosine term, respectively, the summation over n disappears giving

$$
\begin{aligned}
&B_{qs_k} - \mu_0 M_{qs_k} \\
&= \sum_{v=1}^{V} \frac{\mu_k}{\mu_{jv}} \Bigg[\sum_{m=1}^{\infty} \big[(B_{qs_{jv}} - \mu_0 M_{qs_{jv}}) \, \kappa_s(n,m) \\
&\quad + (B_{qc_{jv}} - \mu_0 M_{qc_{jv}}) \, \kappa_c(n,m) \big] \\
&\quad + (B_{q0_{jv}} - \mu_0 M_{q0_{jv}}) \, \kappa_0(n) \Bigg] \Bigg|_{p=h_b}
\end{aligned} \tag{77}
$$

$$
\begin{aligned}
&B_{qc_k} - \mu_0 M_{qc_k} \\
&= \sum_{v=1}^{V} \frac{\mu_k}{\mu_{jv}} \Bigg[\sum_{m=1}^{\infty} \big[(B_{qs_{jv}} - \mu_0 M_{qs_{jv}}) \, \varsigma_s(n,m) \\
&\quad + (B_{qc_{jv}} - \mu_0 M_{qc_{jv}}) \, \varsigma_c(n,m) \big] \\
&\quad + (B_{q0_{jv}} - \mu_0 M_{q0_{jv}}) \, \varsigma_0(n) \Bigg] \Bigg|_{p=h_b}
\end{aligned} \tag{78}
$$

which is a set of equations for every n where the correlation functions κ_s, κ_c, κ_0, ς_s, ς_c, and ς_0 are given by

$$
\kappa_s(n,m) = \frac{s}{\tau_k} \int_{\Delta_{jv}-\Delta_k}^{\Delta_{jv}-\Delta_k+\tau_{jv}} \sin(w_{jv} q_{jv}) \sin(w_k q_k) dq_k \tag{79}
$$

$$
\kappa_c(n,m) = \frac{s}{\tau_k} \int_{\Delta_{jv}-\Delta_k}^{\Delta_{jv}-\Delta_k+\tau_{jv}} \cos(w_{jv} q_{jv}) \sin(w_k q_k) dq_k \tag{80}
$$

$$
\kappa_0(n) = \frac{s}{\tau_k} \int_{\Delta_{jv}-\Delta_k}^{\Delta_{jv}-\Delta_k+\tau_{jv}} \sin(w_k q_k) dq_k \tag{81}
$$

$$
\varsigma_s(n,m) = \frac{s}{\tau_k} \int_{\Delta_{jv}-\Delta_k}^{\Delta_{jv}-\Delta_k+\tau_{jv}} \sin(w_{jv} q_{jv}) \cos(w_k q_k) dq_k \tag{82}
$$

$$
\varsigma_c(n,m) = \frac{s}{\tau_k} \int_{\Delta_{jv}-\Delta_k}^{\Delta_{jv}-\Delta_k+\tau_{jv}} \cos(w_{jv} q_{jv}) \cos(w_k q_k) dq_k \tag{83}
$$

$$
\varsigma_0(n) = \frac{s}{\tau_k} \int_{\Delta_{jv}-\Delta_k}^{\Delta_{jv}-\Delta_k+\tau_{jv}} \cos(w_k q_k) dq_k. \tag{84}
$$

The variable s is equal to 1 when region k has periodic boundary conditions in tangential direction and equal to 2 when region k has Neumann boundary conditions in tangential direction. The solutions of these integrals are given in the Appendix.
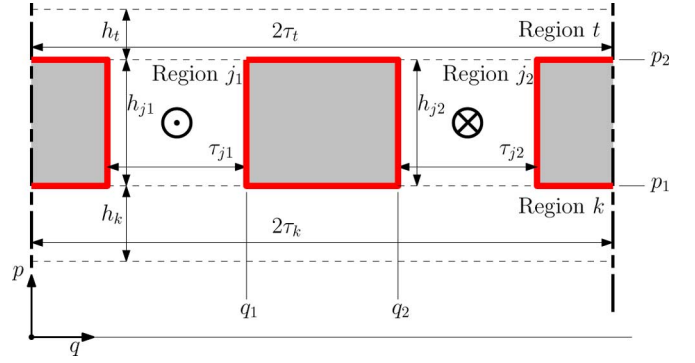

Fig. 10. Conservation of magnetic flux around soft-magnetic blocks surrounded by regions k, j_1, j_2, and t.

D. Conservation of Magnetic Flux

When the source term of a region inhibits a dc term for the magnetization in the tangential direction ($M_{q_0} \neq 0$) or current density in the longitudinal direction ($J_{l_0} \neq 0$), the magnetic flux density in the tangential direction has an extra unknown ($B_0 \neq 0$ for Cartesian and cylindrical coordinate system or $A_0 \neq 0$ for the polar coordinate system).

When this region has a Neumann boundary condition in the normal direction, this extra unknown is solved by the boundary condition given in (57). In the case this region has a continuous boundary condition in the normal direction, this extra term is solved by (65). However, when this region is situated between two other regions with different fundamental period, an extra boundary condition is necessary to solve the extra term. This situation occurs for example with regions II$_i$ of example 3 (Fig. 3) ($M_{q_0} \neq 0$), or with regions j_1 and j_2 of Fig. 10 ($J_{l_0} \neq 0$). In these situations, soft-magnetic "blocks" appear in the structure which are surrounded by four different regions (k, t, j_1, and j_2 in Fig. 10).

The extra boundary condition is given by setting the divergence of the magnetic field to zero (conservation of magnetic flux) around the surface of the soft-magnetic block

$$
\oiint \mathbf{B} \cdot \mathbf{n} dS = 0. \tag{85}
$$

Since only 2-D problems are considered, this surface integral changes to a line integral over the boundary of the block; hence, the boundary condition for every coordinate system is given by

Cartesian:

$$
\begin{aligned}
&\int_{q_1}^{q_2} B_{y_t} dx \bigg|_{y=p_2} - \int_{q_1}^{q_2} B_{y_k} dx \bigg|_{y=p_1} \\
&\quad + \int_{p_1}^{p_2} B_{x_{j2}} dy \bigg|_{x=q_2} - \int_{p_1}^{p_2} B_{x_{j1}} dy \bigg|_{x=q_1} = 0
\end{aligned} \tag{86}
$$

Polar:

$$
\begin{aligned}
&\int_{q_1}^{q_2} B_{r_t} r d\theta \bigg|_{r=p_2} - \int_{q_1}^{q_2} B_{r_k} r d\theta \bigg|_{r=p_1} \\
&\quad + \int_{p_1}^{p_2} B_{\theta_{j2}} dr \bigg|_{\theta=q_2} - \int_{p_1}^{p_2} B_{\theta_{j1}} dr \bigg|_{\theta=q_1} = 0
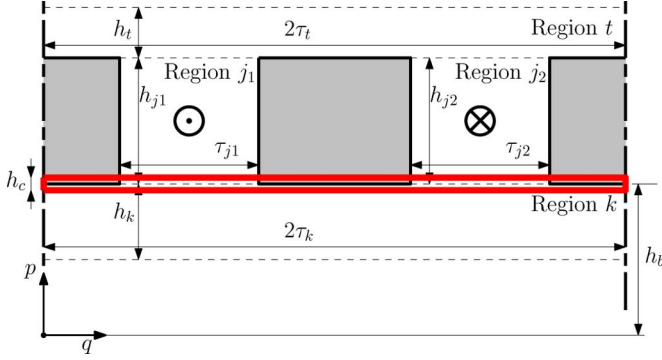\end{aligned} \tag{87}
$$

Fig. 11. Ampère's law around soft-magnetic blocks surrounded by regions k, j_1, j_2, and t.

Fig. 12. Analytical solution of the magnetic flux density distribution for the example in the Cartesian coordinate system.

Cylindrical:

$$\int_{q_1}^{q_2} B_{r_t} r dz \bigg|_{r=p_2} - \int_{q_1}^{q_2} B_{r_k} r dz \bigg|_{r=p_1}$$

$$+ \int_{p_1}^{p_2} B_{z_{j2}} r dr \bigg|_{z=q_2} - \int_{p_1}^{p_2} B_{z_{j1}} r dr \bigg|_{z=q_1} = 0. \quad (88)$$

For a problem concerning V blocks on the same layer, the same number of boundary conditions are obtained. However, only V-1 conditions are independent when the model is periodic. The final independent equation is obtained by applying Ampère's law as explained in the following subsection.

E. Ampère's Law

The final equation for solving the extra terms as explained in the previous section is given by taking the contour integral of the magnetic field strength as shown in Fig. 11. Note that this contour integral could also be applied at the top of regions j_v. The contour integral is given by

$$\lim_{h_c \to 0} \oint H \cdot dl = \oiint J \cdot dS. \quad (89)$$

For every coordinate system, this equation reduces to

$$\frac{2\tau_k}{\mu_k} \left(B_{q0_k} - \mu_0 M_{q0_k} \right) = \frac{\tau_{j1}}{\mu_{j1}} \left(B_{q0_{j1}} - \mu_0 M_{q0_{j1}} \right)$$

$$+ \frac{\tau_{j2}}{\mu_{j1}} \left(B_{q0_{j2}} - \mu_0 M_{q0_{j2}} \right) \bigg|_{p=h_b}. \quad (90)$$

V. FINITE-ELEMENT COMPARISON

A. Example in the Cartesian Coordinate System

In this example, every region has Neumann boundary conditions in the tangential direction; hence, B_{pc} and B_{qs} of every region are zero or the coefficients c_n and d_n are set to zero. The normal magnetization (M_p) of region II only has sine components $(M_{p_0} = 0, M_{pc} = 0)$ and the longitudinal current densities of region IV$_1$ and IV$_2$ only have a dc component ($J_{ls} = 0, J_{lc} = 0$). Neumann boundary conditions (56) and (57) are applied at the bottom of region I$_1$ and I$_2$ and the top of region IV$_1$ and IV$_2$. Furthermore, a continuous boundary condition is applied between region II and III given by (61) and (64). Finally, a combination of Neumann and continuous boundary condition is
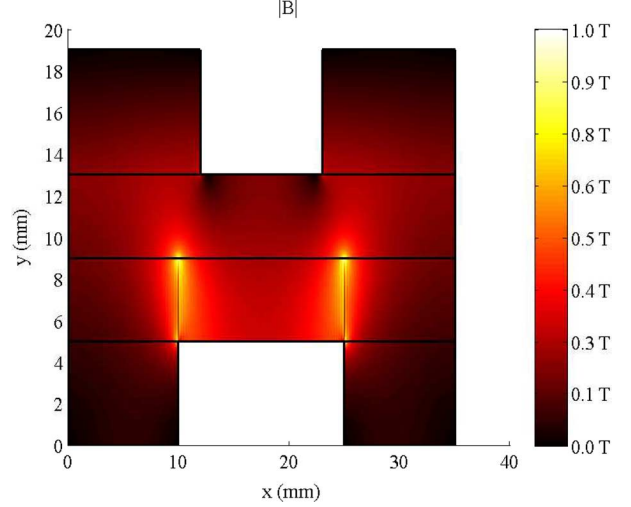
applied at the bottom of region II and the top of region III given by (70) and (78). Solving the set of equations for the parameters given in Table II gives the analytical solution shown in Fig. 12. Comparing this solution with the 2-D finite-element analysis in Fig. 13 shows excellent agreement for every region. The only noticeable discrepancy is at the left and right boundary of the magnet in region II. Only a finite number of harmonics can be taken into account to describe the discontinuous magnetization profile.

B. Example in the Polar Coordinate System

This example considers a rotary actuator with slotted stator. The translator has a quasi-Halbach magnet array; hence, the magnetization profile of region II consists of a normal (M_p) and tangential (M_q) magnetization, only the dc components are zero $(M_{p_0} = 0, M_{q_0} = 0)$. The magnetic field should be zero at the center of the nonmagnetic shaft; hence, the coefficients b_n and d_n of region I are set to zero. Regions IV$_i$ have Neumann boundary conditions in the tangential direction; hence, coefficients c_n and d_n of those regions are zero. The longitudinal current densities of regions IV$_i$ have a dc term and cosine terms; hence, only the sine terms are zero ($J_{ls} = 0$). The amplitudes of the different currents are given by

$$J_a = \hat{J} \cos(\Delta_c) \quad (91)$$

$$J_b = \hat{J} \cos\left(\Delta_c - \frac{2\pi}{3}\right) \quad (92)$$

$$J_c = \hat{J} \cos\left(\Delta_c - \frac{4\pi}{3}\right) \quad (93)$$

where the commutation angle Δ_c is set to $(11\pi)/(60)$ radians in this example. Neumann boundary conditions (56) and (57) are applied at the top of regions IV$_i$. Furthermore, continuous boundary conditions are applied between region I and II and between II and III given by (61), (62), (63), and (64). Finally, a combination of Neumann and continuous boundary condition is applied at the top of region III given by (70), (71), (77), and (78). Solving the set of equations for the parameters given in
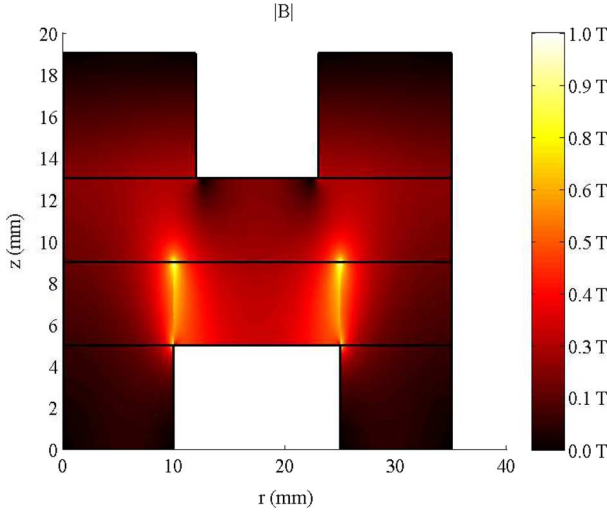
Fig. 13. Finite-element solution of the magnetic flux density distribution for the example in the Cartesian coordinate system.
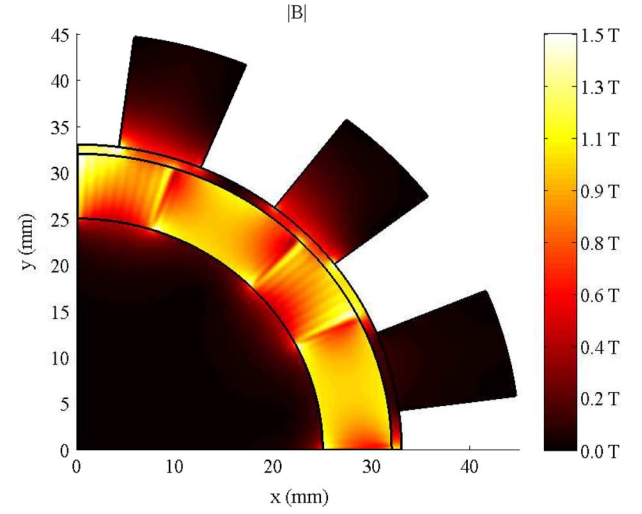
TABLE II
PARAMETERS OF THE MODEL IN THE CARTESIAN COORDINATE SYSTEM

Parameter	Value	Description
K	6	Number of regions
τ_{1i}	10 mm	Width of region I_i
$\tau_{2,3}$	35 mm	Width of region II and III
τ_{4i}	12 mm	Width of region IV_i
h_{1i}	5 mm	Height of region I_i
$h_{2,3}$	4 mm	Height of region II and III
h_{4i}	6 mm	Height of region I_i
$N_{1i,4i}$	50	Harmonics for region I_i and IV_i
$N_{2,3}$	300	Harmonics for region II and III
B_{rem}	1.2 T	Remanent flux density of the magnets
$\mu_{1i,3,4i}$	μ_0	Permeability of region I_i III and IV_i
μ_2	$1.05\,\mu_0$	Permeability of region II
$\hat{J}$	30 A/mm^2	Amplitude of the current density

Table III gives the analytical solution shown in Fig. 14. Again, very good agreement is obtained with the 2-D finite-element analysis shown in Fig. 15. It can be observed that only the magnetic field distribution inside the quasi-Halbach array is difficult to obtain, since again, a high number of harmonics is required to obtain an accurate description of the discontinuous magnetization profile.

C. Example in the Cylindrical Coordinate System

The translator of the actuator under consideration consists of an axial magnetized permanent-magnet array with soft-magnetic pole pieces. Hence, regions II_i have a tangential magnetization with only a dc term ($M_{qs} = 0, M_{qc} = 0$). Furthermore, these regions as well as region IV have Neumann boundary conditions in the tangential direction; hence, coefficients c_n and d_n are zero. The magnetic flux density has to be zero at the center of the axis, setting the coefficients b_n and d_n for region I to zero. Additionally, since region V has infinite height, coefficients a_n and c_n are set to zero since the magnetic field is assumed to be zero at $r = \infty$. A combination of Neumann and continuous boundary conditions is applied at the top and bottom of regions II_i and IV given by (70), (71), (77), and (78). Furthermore, the divergence of the magnetic field is set to zero around 7 of the 8 pole pieces given by (88), since the 8th equation would not

Fig. 14. Analytical solution of the magnetic flux density distribution for the example in the polar coordinate system.
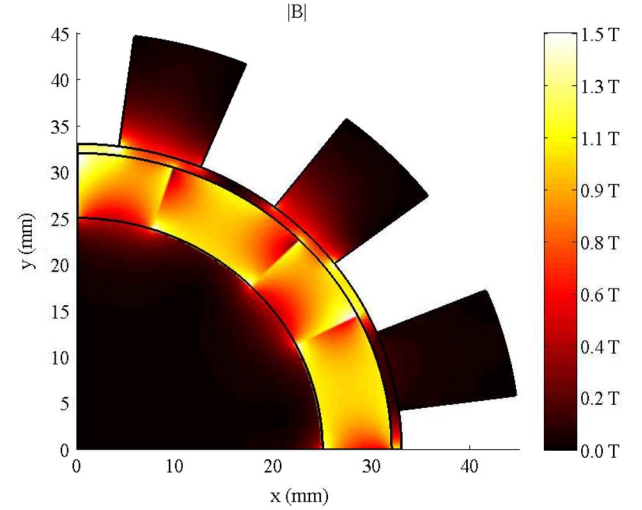

Fig. 15. Finite-element solution of the magnetic flux density distribution for the example in the polar coordinate system.

TABLE III
PARAMETERS OF THE MODEL IN THE POLAR COORDINATE SYSTEM

Parameter	Value	Description
K	6	Number of regions
$2\tau_{1,2,3}$	$\pi/2$	Width of region I, II and III
τ_{4i}	$\pi/12$	Width of region IV_i
α_{mr}	0.4	Ratio of radial magnet width to τ_2
h_1	25 mm	Height of region I
h_2	7 mm	Height of region II
h_3	1 mm	Height of region III
h_{4i}	12 mm	Height of region IV_i
$N_{1,2,3}$	45	Harmonics for region I, II and III
N_{4i}	14	Harmonics for region IV_i
B_{rem}	1.2 T	Remanent flux density of the magnets
$\mu_{1,3,4i}$	μ_0	Permeability of region I, III, IV_i
μ_2	$1.05\,\mu_0$	Permeability of region II
$\hat{J}$	10 A/mm^2	Amplitude of the current density

be an independent equation. The last independent equation is given by applying Ampère's law at the bottom or top of regions II_i given by (90). Solving the set of equations for the parameters given in Table IV gives the analytical solution shown in Fig. 16.
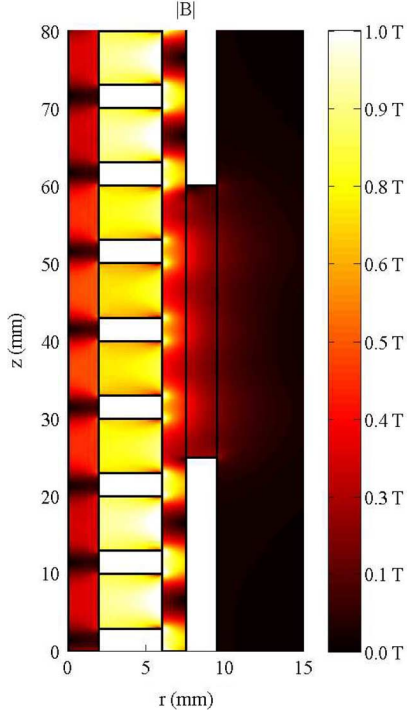
Fig. 16. Analytical solution of the magnetic flux density distribution for the example in the cylindrical coordinate system.
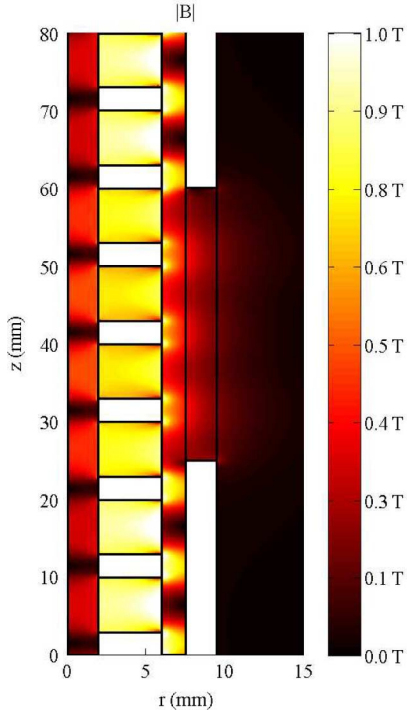

Fig. 17. Finite-element solution of the magnetic flux density distribution for the example in the cylindrical coordinate system.

Again, very good agreement is obtained with the 2-D finite-element analysis shown in Fig. 17. In this case excellent agreement is obtained for every region including the magnets since in this case, in order to describe the magnetization profile, only the dc component is necessary.

TABLE IV
PARAMETERS OF THE MODEL IN THE CYLINDRICAL COORDINATE SYSTEM

Parameter	Value	Description
K	12	Number of regions
$2\tau_{1,3,5}$	80 mm	Width of region I, III and V
τ_{2i}	7 mm	Width of region II$_i$
h_1	2 mm	Height of region I
h_{2i}	4 mm	Height of region II$_i$
h_3	1.5 mm	Height of region III
h_4	2 mm	Height of region IV
$N_{1,3,5}$	120	Harmonics for region I, III and V
N_{2i}	60	Harmonics for region II$_i$
N_4	20	Harmonics for region IV
B_{rem}	1.2 T	Remanent flux density of the magnets
$\mu_{1,3,4,5}$	μ_0	Permeability of region I, III, IV and V
μ_{2i}	$1.05\,\mu_0$	Permeability of region II$_i$

VI. NUMERICAL LIMITATIONS

Modeling techniques which use a meshed geometry will have a limited accuracy related to the density of the mesh. The framework based on Fourier theory exhibits a similar problem in the frequency domain. Therefore, the inaccuracies of the proposed method are all related to the limited amount of harmonics included in the solution. The two reasons for the possibility of including a finite number of harmonics is a limiting computational time and numerical accuracy. For an increased harmonic number, the value of the coefficients a_n and c_n are decreasing while b_n and d_n are increasing. Solving the sets of equations for the boundary conditions results in a system of equations which is ill-conditioned; hence, the solution becomes inaccurate.

This problem can be reduced by including proper scaling of the coefficients a_n, b_n, c_n, and d_n for every region. This is possible in the Cartesian and polar coordinate system since

$$\text{Cartesian:} \quad a_n \frac{e^{wp}}{e^{wp_0}} = a_n e^{w(p-p_0)} \tag{94}$$

$$\text{Polar:} \quad a_n \frac{p^{w-1}}{p_0^{w-1}} = a_n \left(\frac{p}{p_0}\right)^{w-1} \tag{95}$$

for a given normal height p_0. However, this scaling technique cannot be applied for Bessel functions, making problems in the cylindrical coordinate system difficult, if not impossible, to scale.

Limiting the number of harmonics will lead to inaccurate field solutions at discontinuous points in the geometry, especially at the corner points of magnets, current regions, or soft-magnetic material. The correlation technique which is used to satisfy the boundary conditions between regions with different spatial frequencies has drawbacks when only a finite number of harmonics can be considered. In order to illustrate the effect, the analytical field solution is plotted at the boundary between region II$_1$ and region III of the example in the cylindrical coordinate system together with the finite-element solution for the normal magnetic flux density in Fig. 18 and the tangential magnetic field strength in Fig. 19. However, this inaccuracy decays when the field solution is not calculated at the boundaries but close to, for example in the center of region III, as shown in Fig. 20, where very good agreement is obtained. Additionally, the number of harmonics for each region should be chosen carefully, an extensive discussion on the effect of the number of harmonics taken into account is given in [26].
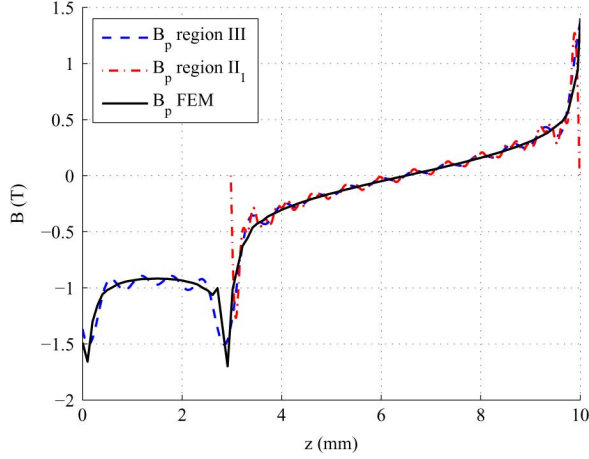
Fig. 18. The normal magnetic flux density component at r = 6 mm for example in the cylindrical coordinate system.
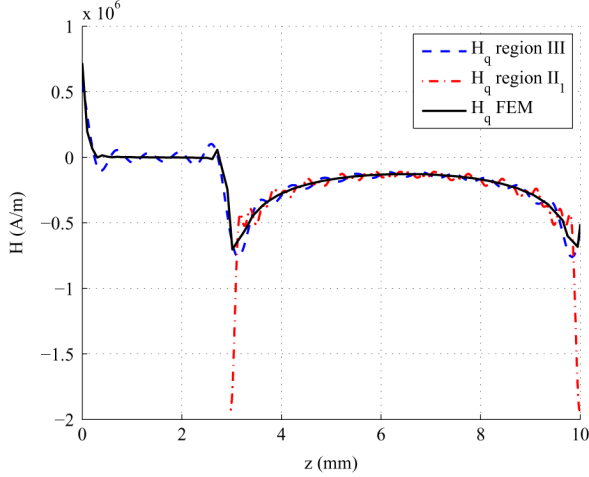

Fig. 19. The tangential magnetic field strength component at r = 6 mm for the example in the cylindrical coordinate system.
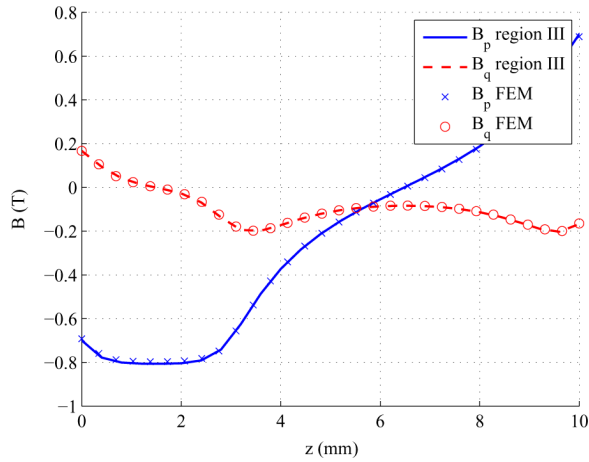

Fig. 20. The field solution at r = 6.75 mm for the example in the cylindrical coordinate system.

A second drawback of this framework are the integrals (51) and (52) in the source functions of the cylindrical coordinate system. Note that the use of these integrals is only necessary when M_{ps}, M_{pc}, J_{ls}, or J_{lc} are nonzero. These integrals are

difficult, if not impossible, to solve analytically and hence are solved numerically. For obtaining the solution by means of solving the set of boundary conditions, only the solution of the source function at the top and bottom of the source region is necessary, hence the amount of numerical integrals is limited. If, however, after obtaining the solution, the magnetic field within the source region has to be obtained, the integrals have to be solved numerically for every radius in consideration.

VII. CONCLUSION

A semianalytical framework for solving the magnetostatic field distribution in 2-D boundary value problems is given for three different coordinate systems. This technique can be applied to any geometry consisting of rectangular regions which exhibits a certain periodicity, or is bound by soft-magnetic material. The source term description and the resulting magnetic field distribution is written in terms of Fourier series. The various boundary conditions are discussed in detail which result in a set of linear equations that solve the total boundary value problem. The framework is applied to various examples in different coordinate systems, and the solutions are verified with 2-D finite-element analyses. Excellent agreement is obtained, which shows the applicability of this model to various electromagnetic actuators and devices. Furthermore, the drawbacks and stability of numerical implementation are discussed.

APPENDIX

$$\varepsilon_s = \frac{2m\tau_k^2[\sin(w_k\Delta) - \cos(m\pi)\sin(w_k(\Delta + \tau_{jv}))]}{\pi\left(m^2\tau_k^2 - n^2\tau_{jv}^2\right)}$$

$$\varepsilon_c = \frac{2m\tau_k^2[\cos(w_k\Delta) - \cos(m\pi)\cos(w_k(\Delta + \tau_{jv}))]}{\pi\left(m^2\tau_k^2 - n^2\tau_{jv}^2\right)}$$

$$\eta_s = \frac{-2n\tau_k\tau_{jv}[\cos(w_k\Delta) - \cos(m\pi)\cos(w_k(\Delta + \tau_{jv}))]}{\pi\left(m^2\tau_k^2 - n^2\tau_{jv}^2\right)}$$

$$\eta_c = \frac{2n\tau_k\tau_{jv}[\sin(w_k\Delta) - \cos(m\pi)\sin(w_k(\Delta + \tau_{jv}))]}{\pi\left(m^2\tau_k^2 - n^2\tau_{jv}^2\right)}$$

$$\kappa_s = \frac{sm\tau_k\tau_{jv}[\sin(w_k\Delta) - \cos(m\pi)\sin(w_k(\Delta + \tau_{jv}))]}{\pi\left(m^2\tau_k^2 - n^2\tau_{jv}^2\right)}$$

$$\kappa_c = -\frac{sn\tau_{jv}^2[\cos(w_k\Delta) - \cos(m\pi)\cos(w_k(\Delta + \tau_{jv}))]}{\pi\left(m^2\tau_k^2 - n^2\tau_{jv}^2\right)}$$

$$\kappa_0 = \frac{s[\cos(w_k\Delta) - \cos(w_k(\Delta + \tau_{jv}))]}{n\pi}$$

$$\varsigma_s = \frac{sm\tau_k\tau_{jv}[\cos(w_k\Delta) - \cos(m\pi)\cos(w_k(\Delta + \tau_{jv}))]}{\pi\left(m^2\tau_k^2 - n^2\tau_{jv}^2\right)}$$

$$\varsigma_c = \frac{sn\tau_{jv}^2[\sin(w_k\Delta) - \cos(m\pi)\sin(w_k(\Delta + \tau_{jv}))]}{\pi\left(m^2\tau_k^2 - n^2\tau_{jv}^2\right)}$$

$$\varsigma_0 = \frac{-s[\sin(w_k\Delta) - \sin(w_k(\Delta + \tau_{jv}))]}{n\pi}$$

where $\Delta = \Delta_{jv} - \Delta_k$ and where s is equal to 1 when region k has periodic boundary conditions in tangential direction and equal to 2 when region k has Neumann boundary conditions in

tangential direction. If $m\tau_k = n\tau_{jv}$, the correlation functions are given by

$$\varepsilon_s = \cos\left(\frac{n\pi\Delta}{\tau_k}\right), \quad \varepsilon_c = -\sin\left(\frac{n\pi\Delta}{\tau_k}\right),$$

$$\eta_s = \sin\left(\frac{n\pi\Delta}{\tau_k}\right), \quad \eta_c = \cos\left(\frac{n\pi\Delta}{\tau_k}\right),$$

$$\kappa_s = \frac{s\tau_{jv}}{2\tau_k}\cos\left(\frac{n\pi\Delta}{\tau_k}\right), \quad \kappa_c = \frac{s\tau_{jv}}{2\tau_k}\sin\left(\frac{n\pi\Delta}{\tau_k}\right),$$

$$\varsigma_s = \frac{s\tau_{jv}}{2\tau_k}\sin\left(\frac{n\pi\Delta}{\tau_k}\right), \quad \varsigma_c = \frac{s\tau_{jv}}{2\tau_k}\cos\left(\frac{n\pi\Delta}{\tau_k}\right).$$

REFERENCES

[1] V. Ostovic, *Dynamics of Saturated Electric Machines*. New York: Springer-Verlag, 1989.

[2] H. C. Roters, *Electromagnetic Devices.*. New York: Wiley, 1941.

[3] G. Akoun and J.-P. Yonnet, "3d analytical calculation of the forces exerted between two cuboidal magnets," *IEEE Trans. Magn.*, vol. MAG-20, no. 5, pp. 1962–1964, Sep. 1984.

[4] G. Xiong and S. Nasar, "Analysis of fields and forces in a permanent magnet linear synchronous machine based on the concept of magnetic charge," *IEEE Trans. Magn.*, vol. 25, no. 3, pp. 2713–2719, May 1989.

[5] B. Hague, *Electromagnetic Problems in Electrical Engineering*. London, U.K.: Oxford Univ. Press, 1929.

[6] J. R. Melcher, *Continuum Electromechanics*. Cambridge, MA: MIT Press, 1981.

[7] N. Boules, "Two-dimensional field analysis of cylindrical machines with permanent magnet excitation," *IEEE Trans. Ind. Appl.*, vol. IA-20, no. 5, pp. 1267–1277, Sep. 1984.

[8] Z. Zhu, D. Howe, E. Bolte, and B. Ackermann, "Instantaneous magnetic field distribution in brushless permanent magnet dc motors. Part I. Open-circuit field," *IEEE Trans. Magn.*, vol. 29, no. 1, pp. 124–135, Jan. 1993.

[9] K. J. Binns, P. J. Lawrenson, and C. W. Trowbridge, *The Analytical and Numerical Solution of Electric and Magnetic Fields*. London, U.K.: Wiley, 1992.

[10] T. A. Driscoll and L. N. Trefethen, *Schwarz-Christoffel Mapping*. Cambridge, U.K.: Cambridge Univ. Press, 2002.

[11] M. Markovic, M. Jufer, and Y. Perriard, "Analyzing an electromechanical actuator by Schwarz-Christoffel mapping," *IEEE Trans. Magn.*, vol. 40, no. 4, pp. 1858–1863, Jul. 2004.

[12] D. Zarko, D. Ban, and T. Lipo, "Analytical calculation of magnetic field distribution in the slotted air gap of a surface permanent-magnet motor using complex relative air-gap permeance," *IEEE Trans. Magn.*, vol. 42, no. 7, pp. 1828–1837, Jul. 2006.

[13] J. M. Jin, *The Finite Element Method in Electromagnetics*, 2nd ed. New York: Wiley, 2002.

[14] L. C. Wrobel and M. H. Aliabadi, *The Boundary Element Method*. New York: Wiley, 2002.

[15] C. J. Carpenter, "Surface-integral methods of calculating forces on magnetized iron parts," *Proc. IEE*, vol. 107C, pp. 19–28, 1959.

[16] J. Coulomb, "A methodology for the determination of global electromechanical quantities from a finite element analysis and its application to the evaluation of magnetic forces, torques and stiffness," *IEEE Trans. Magn.*, vol. MAG-19, no. 6, pp. 2514–2519, Nov. 1983.

[17] J. Coulomb and G. Meunier, "Finite element implementation of virtual work principle for magnetic or electric force and torque computation," *IEEE Trans. Magn.*, vol. MAG-20, no. 5, pp. 1894–1896, Sep. 1984.

[18] A. S. Khan and S. K. Mukerji, "Field between two unequal opposite and displaced slots," *IEEE Trans. Energy Convers.*, vol. 7, no. 1, pp. 154–160, Mar. 1992.

[19] D. Trumper, M. Williams, and T. Nguyen, "Magnet arrays for synchronous machines," in *Conf. Rec. 1993 Ind. Appl. Soc. Annu. Meeting*, Oct. 1993, vol. 1, pp. 9–18.

[20] J. Wang, G. W. Jewell, and D. Howe, "A general framework for the analysis and design of tubular linear permanent magnet machines," *IEEE Trans. Magn.*, vol. 35, no. 3, pp. 1986–2000, May 1999.

[21] J. Wang, D. Howe, and G. Jewell, "Fringing in tubular permanent-magnet machines: Part I. Magnetic field distribution, flux linkage, and thrust force," *IEEE Trans. Magn.*, vol. 39, no. 6, pp. 3507–3516, Nov. 2003.

[22] Z. Liu and J. Li, "Analytical solution of air-gap field in permanent-magnet motors taking into account the effect of pole transition over slots," *IEEE Trans. Magn.*, vol. 43, no. 10, pp. 3872–3883, Oct. 2007.

[23] K. Meessen, B. Gysen, J. Paulides, and E. Lomonova, "Halbach permanent magnet shape selection for slotless tubular actuators," *IEEE Trans. Magn.*, vol. 44, no. 11, pp. 4305–4308, Nov. 2008.

[24] B. Gysen, K. Meessen, J. Paulides, and E. Lomonova, "Semi-analytical calculation of the armature reaction in slotted tubular permanent magnet actuators," *IEEE Trans. Magn.*, vol. 44, no. 11, pp. 3213–3216, Nov. 2008.

[25] *"FLUX2D 10.2 User's Guide,"* Cedrat, Meylan, France, 2008.

[26] S. W. Lee, W. Jones, and J. Campbell, "Convergence of numerical solutions of iris-type discontinuity problems," *IEEE Trans. Microw. Theory Tech.*, vol. 19, no. 6, pp. 528–536, Jun. 1971.